CB No. 5B05

NATIONAL ADVISORY COMMITTEE FOR AERONAUTICS

# WARTIME REPORT

ORIGINALLY ISSUED

April 1945 as
Confidential Bulletin 5B05

## COMPUTATION OF HINGE-MOMENT CHARACTERISTICS OF HORIZONTAL TAILS FROM SECTION DATA

By Robert M. Crane

Ames Aeronautical Laboratory
Moffett Field, Calif.



NACA

WASHINGTON

NATIONAL ADVISORY COMMITTEE FOR AERONAUTICS

CONFIDENTIAL BULLETIN

# COMPUTATION OF HINGE-MOMENT CHARACTERISTICS OF HORIZONTAL TAILS FROM SECTION DATA

By Robert M. Crane

## SUMMARY

A study of data from various wind-tunnel tests of horizontal tail surfaces was made to determine the accuracy with which section data can be used to estimate the hinge-moment characteristics of control surfaces of finite span. The study consisted of a comparison between the variation of elevator hinge moments with elevator deflection and with airplane pitching moment, as estimated from data obtained in two-dimensional flow, and that variation measured experimentally on 16 different horizontal tails mounted on wind-tunnel models of complete airplanes. The method used in applying section data to the evaluation of three-dimensional characteristics is outlined, and summary curves showing the variation of the major parameters with control-surface chord, balance chord, and trailing-edge angle are presented. It is demonstrated that the three-dimensional hinge-moment characteristics of tail surfaces can be derived from existing section data with an accuracy which is within the tolerance required in preliminary design.

## INTRODUCTION

Considerable data on the characteristics of large-chord flaps have been obtained (references 1 to 11), which establish the effect of the major variables (flap chord, balance chord, nose shape, nose gap, etc.) on the section aerodynamic characteristics of airfoils. The question has arisen on occasion, as to the degree of accuracy with which these data can be applied to the estimation of the characteristics of control surfaces in three-dimensional flow. This question is particularly pertinent as applied to the horizontal or vertical tail surfaces of complete airplanes, since these surfaces (as distinguished from ailerons) are subjected to mutual interferences, fuselage interference, and are of relatively low aspect ratio, so that the differences caused by these "secondary" effects might be so large as to preclude the use of section data for anything but the most approximate estimates.

In order to shed some light on this problem, the experimentally measured hinge-moment and pitching-moment characteristics of 16 different horizontal tail surfaces mounted on complete airplane models have been compiled and are compared with characteristics estimated from data obtained in two-dimensional flow. This study has taken the form of the comparison of hinge-moment characteristics as defined by the variation of elevator hinge moments with elevator angle, with tail angle of attack, and with airplane pitching moments. The types of aerodynamic balance considered in the present investigation include internally sealed nose balance and unshrouded nose overhang balance.

No consideration has been given to shielded or unshielded horn-type balances. The data presented have been confined to those obtained at zero angle of attack of the tail, but are typical of the range of angles of attack encountered by a tail in normal flight. Considerations were limited to elevator deflections where stall is absent (characteristics remain linear), and all the experimental data were determined in the absence of operating propellers. These restrictions, however, do not prevent application of the conclusions to the flight conditions where the elevator stick forces are normally most critical; namely, accelerated maneuvers at high speed (where the elevator deflections are normally small and the slipstream effects are negligible).

In order to facilitate the application of section data to control surfaces on which the important geometric variables were different from the basic data available, a systematic method of application was developed. This method and an illustrative example on one of the tail surfaces are outlined in the section Method, and the results of application of this method to 16 tail surfaces are considered in the section Discussion.

## SYMBOLS

The symbols used in this paper are defined as follows:

| | |
|---|---|
| $c_l$ | airfoil section lift coefficient $\left(\frac{l}{qc}\right)$ |
| $C_L$ | airfoil lift coefficient $\left(\frac{L}{qS}\right)$ |
| $c_h$ | control-surface section hinge-moment coefficient $(h/qc_f^2)$ |
| $C_h$ | elevator hinge-moment coefficient $\left(\frac{H}{qS_e\bar{c}_e}\right)$ |
| $C_m$ | airplane pitching-moment coefficient $\left(\frac{M}{qS_w(M.A.C.)}\right)$ |

where

| | |
|---|---|
| $l$ | airfoil section lift |
| L | airfoil lift |
| h | control-surface section hinge moment |
| H | elevator hinge moment |
| M | airplane pitching moment about center of gravity |
| c | chord of airfoil with control surface neutral, mean geometric chord of horizontal tail |
| M.A.C. | mean aerodynamic chord of wing |
| $c_f$ | chord of control surface aft of hinge line |
| $c_e$ | mean geometric chord of elevator aft of hinge line |
| $\bar{c}_e$ | root-mean-square chord of elevator aft of hinge line |
| $S_w$ | area of wing |
| $S_e$ | area of elevator aft of hinge line |
| q | dynamic pressure of air stream $(\frac{1}{2}\rho V^2)$ |

In addition to these the following symbols have been employed:

| | |
|---|---|
| $\alpha$ | angle of attack of horizontal tail or airfoil |
| $\delta$ | control-surface deflection with respect to the airfoil |
| $l_{h_e}$ | elevator tail length (horizontal distance from center of gravity of airplane to the center of pressure of the tail load due to elevator deflection) |
| $S_{H_e}$ | horizontal tail area affected by the elevator |
| A | aspect ratio of horizontal tail |
| $\Phi$ | trailing-edge angle of control surface |
| $c_{l_\alpha}$ | $(\partial c_l/\partial\alpha)_\delta$ |
| $C_{L_\alpha}$ | $(\partial C_L/\partial\alpha)_\delta$ |
| $\alpha_\delta$ | $(\partial\alpha/\partial\delta)_{c_l}$ |
| $c_{l_\delta}$ | $(\partial c_l/\partial\delta)_\alpha$ |
| $c_{h_\alpha}$ | $(\partial c_h/\partial\alpha)_\delta$ |
| $C_{h_\alpha}$ | $(\partial C_h/\partial\alpha)_\delta$ |
| $c_{h_\delta}$ | $(\partial c_h/\partial\delta)_\alpha$ |
| $C_{h_\delta}$ | $(\partial C_h/\partial\delta)_\alpha$ |

The subscripts outside the parentheses indicate the factors held constant during the measurement of the parameters.

## METHOD

The influence of the following factors has been included in the calculation of the parameters $C_{h_\delta}$, $C_{h_\alpha}$, and $(\partial C_h/\partial C_m)_\alpha$.

(1) The elevator chord aft of the hinge line

(2) The elevator balance chord forward of the hinge line

(3) The elevator nose gap

(4) The elevator nose shape

(5) The airfoil section of the horizontal tail, especially as it affects $\Phi$, the included angle between the upper and lower surfaces at the trailing edge of the airfoil

(6) The aspect ratio of the horizontal tail

The data of references 1 to 11 are used to establish the effects of the first five of the above variables on the section characteristics. These data were collected subsequently and presented in reference 12. To facilitate the use of these section data, they have been fully corrected for tunnel-wall effect and are presented in figures 1 to 8 in a form suitable for the present application. In the application of these data the following assumptions have been made:

(1) The variation of the section characteristics $\alpha_\delta$, $c_{h_\delta}$, and $c_{h_\alpha}$ with percent chord will be independent of the section profile. This assumption permits the variation given in reference 1, which was determined from tests of an NACA 0009 airfoil with various chord flaps, to be applied to any other section profile.

(2) The hinge-moment parameter increments due to changes in trailing-edge angle are independent of flap-chord ratio and have the following value:

$$\frac{\Delta c_{h_\alpha}}{c_{l_\alpha} \Delta \Phi} = 0.0050$$

$$\frac{\Delta c_{h_\delta}}{c_{l_\delta} \Delta \Phi} = 0.0078$$

The data of figure 2 of reference 11 have been reproduced in figure 7 of this report in a form more suitable for the present application. Data from additional tests on beveled control surfaces (references 13, 14, and 15) have been included to demonstrate the scatter of the experimental points around the proposed correlation curve. It is obvious that all the factors which influence the effect of the trailing-edge angle on the hinge-moment parameters have not been included in these curves. Since the increments in trailing-edge angle needed in this report are small (no beveled trailing-edge control surfaces considered herein), no attempt has been made to determine a more accurate correlation method, and an average value has been chosen from the existing data.

(3) The hinge-moment parameters of balanced flaps vary in the same manner with ratio of flap chord to airfoil chord as do the parameters for plain flaps. This assumption is made for the sake of expedience. It lacks experimental verification, but the effect of the possible error on the final results is not large.

(4) The interference effects due to the fuselage or vertical tail do not affect $C_{h_\alpha}$, $C_{h_\delta}$, or $(\partial C_h/\partial C_m)_\alpha$. It was assumed that there was no carry-over of lift over the center section of the horizontal tail.

In the application of these section data to finite-span control surfaces, the lifting-line theory and the assumption of an elliptic span loading have been used as a basis for estimating the effect of aspect ratio on the section lift and section hinge-moment characteristics. These assumptions enable the parameters $(\partial\alpha/\partial\delta)_{c_l}$, $(\partial c_h/\partial c_l)_\delta$, and $(\partial c_h/\partial\delta)_{c_l}$ to be treated as independent of aspect ratio and spanwise location. No account has been taken of the variation of the induced angle along the span due to the actual spanwise loading,[1] and the refinements of lifting-surface theory have not been applied.[2]

---

[1]The finite-span hinge moments for two of the representative horizontal tails considered in the present analysis have been computed by taking into account the aerodynamic induction due to the actual spanwise loading. The very small increase in accuracy of these computations over those in which an elliptic loading was considered did not warrant the use of this refinement.

[2]Since the downwash actually varies along the chord, an error is introduced in the calculation of the hinge moments by lifting-line theory because the hinge moments are a function of the distribution as well as the magnitude of the resultant pressure. Preliminary calculations of the chordwise distribution of lift indicate an additional aspect-ratio correction which increases (algebraically) the hinge-moment-coefficient slopes. This limitation of lifting-line theory as applied to the calculation of finite-span hinge moments has been previously reported in reference 16.

The method of application divides itself into the following steps:

A. Computation of the effects of aerodynamic balance

1. Internal seal

(a) Estimate of parameters of plain sealed control surfaces (figs. 1 to 4)

(b) Computation of hinge-moment increments due to balance (fig. 5)

(c) Computation of the characteristic with balance ((a) plus (b))

2. External overhang balance

(a) Interpolation of parameters for elevator balance chord, nose gap and nose shape (figs. 1 to 4)

B. Adjustment of section parameters for effect of control-surface chord (fig. 6)

C. Adjustment of section parameters for effect of trailing-edge angle (fig. 7)

D. Application of final section parameters to three-dimensional flow

## ILLUSTRATIVE EXAMPLE

To illustrate the method, the following example has been carried out on the elevator of the horizontal tail of airplane A, the characteristics of which are shown in figure 9. This horizontal tail has a 0.12-chord-thick airfoil section for which the trailing-edge angle is 14.6°. The control-surface chord ratio has a constant value of 0.40 and the elevator is equipped with an overhanging balance of $0.25c_e$. The nose shape of the balance closely corresponds to the medium nose shape of references 2 to 8 and the nose gap is 0.005c.

<u>A-2.- Characteristics of a 0.30-chord flap with a $0.25c_e$ medium nose balance with 0.005c gap on an NACA 0009 airfoil.</u>- Figure 1 presents the section characteristics of an

NACA 0009 airfoil with a medium-nose profile overhanging balance. From these data, the section parameters for an airfoil equipped with a 0.30-chord flap with $0.25c_e$ medium nose balance with 0.005c gap are as follows:

$$c_{l_\alpha} = 0.091$$

$$\alpha_\delta = -0.56$$

$$c_{h_\alpha} = -0.0043$$

$$c_{h_\delta} = -0.0078$$

B.- Adjustment of section parameters for control-surface chord.- These values for a 0.30-chord flap are corrected to 0.40-chord flap by the data presented in figure 6.

$$c_{l_\alpha} = 0.091$$

$$\alpha_\delta = -0.56 \times \frac{0.72}{0.60} = -0.67$$

$$c_{h_\alpha} = -0.0043 \times \frac{0.0084}{0.0060} = -0.0060$$

$$c_{h_\delta} = -0.0078 \times \frac{0.0133}{0.0120} = -0.0087$$

C.- Adjustment of section data for trailing-edge angle.- To the preceding values an adjustment is made for trailing-edge angle $\Phi$. The trailing-edge angle of the NACA 0009 airfoil is 11°, while that of the subject airfoil is 14.6°. From figure 7 for a $c_{l_\alpha}$ of 0.091, a $c_{l_\delta}$ of $0.67 \times 0.091 = 0.061$ and a $\Delta\Phi$ of 3.6°.

$$\Delta c_{h_\alpha} = 0.0050 \times 0.091 \times 3.6 = 0.0017$$

$$\Delta c_{h_\delta} = 0.0078 \times 0.061 \times 3.6 = 0.0017$$

Adjusting the previous parameters, the section characteristics of the horizontal tail of airplane A are obtained.

$$c_{l_\alpha} = 0.091$$

$$\alpha_\delta = -0.67$$

$$c_{h_\alpha} = -0.0043$$

$$c_{h_\delta} = -0.0070$$

<u>D.- Application of the final section parameters to the finite span</u>.- These data are adjusted for a finite aspect ratio by the following relationships:

$$C_{L_\alpha} = p\left[\frac{c_l{}'_\alpha}{1 + \left(\frac{57.3 r c_{l_\alpha}}{\pi A}\right)}\right]$$

(Values of $p$ and $r$ are plotted in fig. 8.)

$$C_{h_\alpha} = c_{h_\alpha}\frac{C_{L_\alpha}}{c_{l_\alpha}}$$

$$C_{h_\delta} = c_{h_\delta} + \alpha_\delta\left(c_{h_\alpha} - C_{h_\alpha}\right)$$

$$\left(\frac{\partial C_h}{\partial C_m}\right)_\alpha = \frac{C_{h_\delta}}{C_{L_\alpha}\alpha_\delta V_e}$$

where $V_e$ is the elevator volume and is equal to $\frac{l_{h_e}}{\text{M.A.C.}}\,\frac{S_{H_e}}{S_W}$

Applying the section parameters to these equations, the aerodynamic characteristics of the horizontal tail of airplane A are obtained:

$$C_{L_\alpha} = 0.059$$

$$\alpha_\delta = -0.067$$

$$C_{H_\alpha} = -0.0028$$

$$C_{h_\delta} = -0.0060$$

$$\left(\frac{\partial C_h}{\partial C_m}\right)_\alpha = 0.270$$

Comparison with experimental results.- This predicted variation of $C_h$ with $\delta$ is shown in figure 9. On the same axis, data obtained on a 1/5-scale model of airplane A are plotted. It is observed that the data obtained in three-dimensional flow indicate a $C_{h_\delta}$ of $-0.0052$, a deviation from the estimated value of 0.0008.

The computed value of $\left(\frac{\partial C_h}{\partial C_m}\right)_\alpha$ is plotted in figure 9, and comparison is afforded between this value and that measured on the 1/5-scale model. For this airplane the difference between the computed and measured values of $\left(\frac{\partial C_h}{\partial C_m}\right)_\alpha$ is 0.010.

The value of $C_{h_\alpha}$ was not measured experimentally, but it may be determined from the original data by means of the following relationship:

$$C_{h_\alpha} = \frac{\partial C_h}{\partial C_L} \times \frac{\partial C_m/\partial i_t}{(\partial C_m/\partial C_L)_T}$$

where

$C_L$ airplane lift coefficient

$i_t$ tail incidence

and

$$\left(\frac{\partial C_m}{\partial C_L}\right)_T = \left(\frac{\partial C_m}{\partial C_L}\right)_{\text{tail on}} - \left(\frac{\partial C_m}{\partial C_L}\right)_{\text{tail off}}$$

Applying the relationship to the data of airplane A, $C_{h_\alpha}$ is found to have an experimental value of −0.0012. The computed value of this slope was −0.0028, a deviation of 0.0016.

## DISCUSSION

Similar calculations have been made on the horizontal tail surfaces of 15 other airplanes. The estimated and measured values of $C_{h_\delta}$ and $(\partial C_h/\partial C_m)_\alpha$ are plotted in figures 9 to 24, and are tabulated in table I. All values are presented at the angle of attack at which the tail is subjected to zero lift (elevator undeflected) with power off.

The correlation of $C_{h_\delta}$ is very good in the majority of the cases considered, the scatter of the experimental points about the computed curves being, in most instances, about equal to normal experimental scatter. For 12 of the 16 tail surfaces included in the analysis, the difference between the predicted and the measured values of $C_{h_\delta}$ was between $\pm 0.0008$. This difference is equivalent to the balance effect of less than $\pm 3$ percent $c_e$ nose balance on a closely balanced elevator. The deviation of the slope in the remaining cases was −0.0013 or less. For 11 of the 16 cases considered, the computed value of $C_{h_\delta}$ was too negative, indicating the necessity of a larger correction to $c_{h_\delta}$ due to aspect ratio.

Due to the nonlinearity of the relationship involved, it is difficult to establish an experimental value of $C_{h_\alpha}$. For the cases considered, the deviation between the experimental and the estimated values ranged from 0.0009 to −0.0020. For all the airplanes except three, the computed value of $C_{h_\alpha}$ was algebraically smaller than the value measured in the wind tunnel. This is in accord with the additional aspect-ratio correction to $c_{h_\alpha}$ predicted from a consideration of the chordwise distribution of the resultant pressure.

The deviation between the measured and computed values of $\left(\frac{\partial C_h}{\partial C_m}\right)_\alpha$ was less than 0.060 in 12 of the 15 cases considered and, with a single exception, was less than 0.079 in the remaining cases. In the single case where a very marked difference exists between the measured and computed values (airplane N), the cause is the exceptionally low elevator effectiveness $(\partial C_m/\partial \delta_e)$ determined experimentally. In five of the fifteen cases, a better correspondence would have been obtained if some carry-over of lift had been assumed across the fuselage. However, the other 10 cases indicate that the assumption of no-lift carry-over gives the best average results. It would appear that $C_{h_\delta}$ can be predicted with greater accuracy than can $(\partial C_h/\partial C_m)_\alpha$.

In order to estimate the magnitude of the error which would result from the use of these estimated hinge-moment data in the calculation of airplane stick forces in accelerated flight, computations have been made of the stick force per g on a typical pursuit airplane due to the discrepancy between the calculated and the experimental values of the hinge-moment parameters. The equations used in this analysis and the assumed airplane characteristics are indicated in the appendix. These airplane characteristics are believed typical for a modern high-speed airplane having a span of approximately 42 feet and a gross weight of 10,000 pounds. Results of these calculations are listed in table I. For nine of the fifteen horizontal tails considered in the analysis, the stick force per g due to the difference between the estimated and the measured hinge-moment slopes was less than 4 pounds. The stick force per g in the remaining cases varied from 5.3 to 16.4. In all cases except seven, the stick force per g would have been underestimated by using the computed hinge-moment data.

In the application of these data to a full-scale airplane, a very important variable exists for which few data are available, namely, the effect of Mach number. All the data presented herein have been obtained at a Mach number of less than 0.2. Tests made at high speeds have indicated Mach number effects on the hinge-moment parameters which are a function of several variables. Among these variables are the trailing-edge angle of the control surface, the amount of nose overhang, the profile of the nose balance, and the nose-balance gap. In most cases, increasing Mach number tends to increase algebraically both $C_{h_\delta}$ and $C_{h_\alpha}$.

This overbalancing effect of Mach number on $C_{h_\delta}$ increases with increasing trailing-edge angle, with increasing nose overhang, and with increasing nose-balance bluntness. In one case of a beveled trailing-edge control surface ($\Phi = 23°$) with a $0.35c_e$ unsealed nose balance, increasing the Mach number from 0.2 to 0.8 resulted in a $\Delta C_{h_\delta}$ of 0.0065. Another example is that of a normal-profile elevator ($\Phi = 13°$) with a $0.40c_e$ blunt-nose balance for which the increase in $C_{h_\delta}$ due to increasing Mach number from 0.2 to 0.8 amounted to 0.0035.

A need exists for a systematic investigation of the effects of Mach number on control-surface hinge moments. Examination of data which are available indicates that the least Mach number effect can be expected for control surfaces which are not bulged or beveled and have either no balance or a sealed internal balance.

## CONCLUDING REMARKS

It is concluded from the foregoing comparisons that the hinge-moment characteristics of tail surfaces can be derived from existing section data with an accuracy well within the tolerance required in preliminary design. It is acknowledged that the effect of other factors, such as fabric distortion and high Mach number, may influence to a large extent the final airplane stick forces.

The utilization of lifting-line theory introduces an error in the application of section hinge-moment data to finite-span control surfaces. An additional aspect-ratio correction to the hinge moments due to the chordwise distribution of downwash is indicated. This correction will tend to increase (algebraically) the elevator hinge moments, thus increasing the accuracy to which finite-span hinge-moment characteristics may be predicted from section data.

Ames Aeronautical Laboratory,
National Advisory Committee for Aeronautics,
Moffett Field, Calif., Oct. 9, 1944.

## APPENDIX

The following equation has been developed to define the variation of elevator stick force with normal acceleration for an airplane in steady turning flight:

$$\Delta f = \frac{f}{C_h q}\left[\left\{\left(\frac{\partial C_h}{\partial C_L}\right)_\delta + \left(\frac{\partial C_h}{\partial \delta}\right)_{C_L} \frac{(\partial C_m/\partial C_L)\delta}{-(\partial C_m/\partial \delta_e)C_l}\right\} l_w\ (n-1)\right.$$

$$\left. + 2.192\left(\frac{n^2-1}{n}\right) l_h\sigma \left\{\left(\frac{\partial C_h}{\partial i_t}\right)_\alpha + \left(\frac{\partial C_h}{\partial \delta}\right)_\alpha \frac{(\partial C_m/\partial i_t)_\alpha}{-(\partial C_m/\partial \delta)_\alpha}\right\}\right]$$

where all symbols have been previously defined except

$f$ elevator stick force

$l_w$ wing loading, pounds per square foot

$n$ normal acceleration

$l_h$ horizontal tail length (distance from airplane center of gravity to center of pressure of horizontal tail)

$\sigma$ density ratio, $\frac{\rho}{\rho_o}$

$C_L$ and $\alpha$ refer to the airplane

The following values of the above variables have been assumed as typical for a modern pursuit airplane:

$$\left(\frac{\partial C_m}{\partial C_L}\right)_\delta = -0.16$$

$$\left(\frac{\partial C_m}{\partial \delta_e}\right)_{C_L} = -0.016$$

$$l_w = 35 \text{ pounds per square foot}$$

$$l_h = 20 \text{ feet}$$

$$\sigma = 0.7385 \text{ (10,000 ft altitude)}$$

$$\left(\frac{\partial C_m}{\partial i_t}\right)_\alpha = -0.032$$

$$\left(\frac{\partial C_m}{\partial C_L}\right)_{\text{tail off}} = 0.04$$

$$\frac{f}{C_{hq}} = 20$$

$$\left(\frac{\partial C_h}{\partial C_L}\right)_\delta = \left(\frac{\partial C_h}{\partial i_t}\right)_{C_L} \frac{\left(\frac{\partial C_m}{\partial C_L}\right)_\delta - \left(\frac{\partial C_m}{\partial C_L}\right)_{\text{tail off}}}{(\partial C_m/\partial i_t)_{C_L}}$$

$$= 6.25 \left(\frac{\partial C_h}{\partial i_t}\right)_{C_L}$$

For the sake of simplicity it has been assumed that

$$\left(\frac{\partial C_h}{\partial \delta_e}\right)_{C_L} = \left(\frac{\partial C_h}{\partial \delta_e}\right)_\alpha$$

$$\left(\frac{\partial C_h}{\partial i_t}\right)_{C_L} = \left(\frac{\partial C_h}{\partial i_t}\right)_\alpha$$

$$\left(\frac{\partial C_m}{\partial i_t}\right)_{C_L} = \left(\frac{\partial C_m}{\partial i_t}\right)_\alpha$$

$$\left(\frac{\partial C_m}{\partial \delta_e}\right)_{C_L} = \left(\frac{\partial C_m}{\partial \delta_e}\right)_\alpha$$

Applying the above values, the stick force required to attain a 2g normal acceleration in steady turning flight may be written as

$$f = 5350 \frac{\partial C_h}{\partial i_t} - 8940 \frac{\partial C_h}{\partial \delta}$$

REFERENCES

1. Ames, Milton B., Jr., and Sears, Richard I.: Determination of Control-Surface Characteristics from NACA Plain-Flap and Tab Data. NACA Rep. No. 721, 1941.

2. Sears, Richard I.: Wind-Tunnel Investigation of Control-Surface Characteristics. I - Effect of Gap on the Aerodynamic Characteristics of an NACA 0009 Airfoil with a 30-Percent-Chord Plain Flap. NACA ARR, June 1941.

3. Sears, Richard I., and Hoggard, H. Page, Jr.: Wind-Tunnel Investigation of Control-Surface Characteristics. II - A Large Aerodynamic Balance of Various Nose Shapes with a 30-Percent-Chord Flap on an NACA 0009 Airfoil. NACA ARR, Aug. 1941.

4. Ames, Milton B., Jr.: Wind-Tunnel Investigation of Control Surface Characteristics. III - A Small Aerodynamic Balance of Various Nose Shapes Used with a 30-Percent-Chord Flap on an NACA 0009 Airfoil. NACA ARR, Aug. 1941.

5. Ames, Milton B., Jr., and Eastman, Donald R., Jr.: Wind-Tunnel Investigation of Control-Surface Characteristics. IV - A Medium Aerodynamic Balance of Various Nose Shapes Used with a 30-Percent-Chord Flap on an NACA 0009 Airfoil. NACA ARR, Sept. 1941.

6. Sears, Richard I., and Liddell, Robert B.: Wind-Tunnel Investigation of Control-Surface Characteristics. VI - A 30-Percent-Chord Plain Flap on the NACA 0015 Airfoil. NACA ARR, June 1942.

7. Sears, Richard I., and Hoggard, H. Page, Jr.: Wind-Tunnel Investigation of Control-Surface Characteristics. VII - A Medium Aerodynamic Balance of Two Nose Shapes Used with a 30-Percent-Chord Flap on an NACA 0015 Airfoil. NACA ARR, July 1942.

8. Sears, Richard I., and Gillis, Clarence L.: Wind-Tunnel Investigation of Control-Surface Characteristics. VIII - A Large Aerodynamic Balance of Two Nose Shapes Used with a 30-Percent-Chord Flap on an NACA 0015 Airfoil. NACA ARR, July 1942.

9. Hoggard, H. Page, Jr.: Wind-Tunnel Investigation of Control-Surface Characteristics. X - A 30-Percent-Chord Plain Flap with Straight Contour on the NACA 0015 Airfoil. NACA ARR, Sept. 1942.

10. Sears, Richard I., and Hoggard, H. Page, Jr.: Wind-Tunnel Investigation of Control-Surface Characteristics. XI - Various Large Overhang and Internal-Type Aerodynamic Balances for a Straight-Contour Flap on the NACA 0015 Airfoil. NACA ARR, Jan. 1943.

11. Purser, Paul E., and Gillis, Clarence L.: Preliminary Correlation of the Effects of Beveled Trailing Edges on the Hinge-Moment Characteristics of Control Surfaces. NACA CB No. 3E14, 1943.

12. Sears, Richard I.: Wind-Tunnel Data on the Aerodynamic Characteristics of Airplane Control Surfaces. NACA ACR No. 3L08, 1943.

13. Purser, Paul E., and Riebe, John M.: Wind-Tunnel Investigation of Control-Surface Characteristics. XV - Various Contour Modifications of a 0.30-Airfoil-Chord Plain Flap on an NACA 66(215)-014 Airfoil. NACA ACR No. 3L20, 1943.

14. Lockwood, Vernard E.: Wind-Tunnel Investigation of Control-Surface Characteristics. XVII - Beveled Trailing-Edge Flaps of 0.20, 0.30, and 0.40 Airfoil Chord on an NACA 0009 Airfoil. NACA ACR No. L4D12, 1944.

15. Crane, Robert M., and Holtzclaw, Ralph W.: Wind-Tunnel Investigation of Ailerons on a Low-Drag Airfoil. II - The Effect of Thickened and Beveled Trailing Edges. NACA ACR No. 4A15, 1944.

16. Swanson, Robert S., and Gillis, Clarence L.: Limitations of Lifting-Line Theory for Estimation of Aileron Hinge-Moment Characteristics. NACA CB No. 3L02, 1943.

TABLE I

COMPARISON OF CALCULATED AND EXPERIMENTAL HINGE-MOMENT PARAMETERS

| Airplane Model | $Ch_\delta$ | | $Ch_\alpha$ | | $(\partial C_h/\partial C_m)_\alpha$ | | $\Delta C_{h_\delta}$ [1] | $\Delta C_{h_\alpha}$ [1] | $\Delta\left(\frac{\partial C_h}{\partial C_m}\right)_\alpha$ [1] | $\Delta f$ [2] |
|---|---|---|---|---|---|---|---|---|---|---|
| | Calcu-lated | Experi-mental | Calcu-lated | Experi-mental | Calcu-lated | Experi-mental | | | | |
| A | -0.0060 | -0.0052 | -0.0028 | -0.0012 | 0.270 | 0.280 | -0.0008 | -0.0016 | -0.010 | -1.4 |
| B | -.0061 | -.0060 | -.0019 | -.0024 | .296 | .256 | -.0001 | .0005 | .040 | 3.5 |
| C | -.0031 | -.0018 | -.0014 | -.0023 | .150 | .071 | -.0013 | .0009 | .079 | 16.4 |
| D | -.0051 | -.0038 | -.0020 | 0 | .213 | .200 | -.0013 | -.0020 | .013 | .9 |
| E | -.0024 | -.0016 | -.0009 | -.0002 | .119 | .085 | -.0008 | -.0007 | .034 | 3.3 |
| F | -.0027 | -.0029 | -.0010 | -.0010 | .152 | .160 | .0002 | 0 | -.008 | -1.8 |
| G | -.0024 | -.0024 | -.0009 | -.0006 | .130 | .130 | 0 | -.0003 | 0 | -1.6 |
| H | -.0054 | -.0043 | -.0021 | -.0010 | .303 | .270 | -.0011 | -.0011 | .033 | 3.9 |
| J | -.0049 | -.0036 | -.0018 | -.0008 | .280 | .245 | -.0013 | -.0010 | .035 | 6.2 |
| K | -.0094 | -.0086 | -.0043 | -.0026 | .360 | .305 | -.0008 | -.0017 | .055 | -1.9 |
| L | -.0050 | -.0054 | -.0010 | -.0002 | .304 | .364 | .0004 | -.0008 | -.060 | -7.9 |
| M | -.0024 | -.0032 | -.0002 | 0 | .134 | .200 | .0008 | -.0002 | -.066 | 8.2 |
| N | -.0066 | -.0063 | -.0007 | .0008 | .306 | .500 | -.0003 | -.0015 | -.194 | -5.3 |
| O | .0002 | .0002 | .0008 | .0007 | -.008 | 0 | 0 | -.0001 | -.008 | .5 |
| P | .0025 | .0032 | ------- | ------- | -.103 | -.130 | -.0007 | ------- | .027 | ------- |
| Q | -.0011 | -.0010 | -.0019 | -.0006 | ------- | ------- | -.0001 | -.0013 | ------- | -6.1 |

[1]Calculated value of slope minus experimental value of slope.

[2]Stick force per g of normal acceleration due to $\Delta C_{h_\alpha}$ and $\Delta C_{h_\delta}$, $\Delta f = 5350\ \Delta C_{h_\alpha} - 8940\ \Delta C_{h_\delta}$

NOTE.- When $\Delta C_{h_\delta}$ and $\Delta C_{h_\alpha}$ possess the same algebraic sign, the stick forces due to the hinge-moment increments are compensative.

A-11

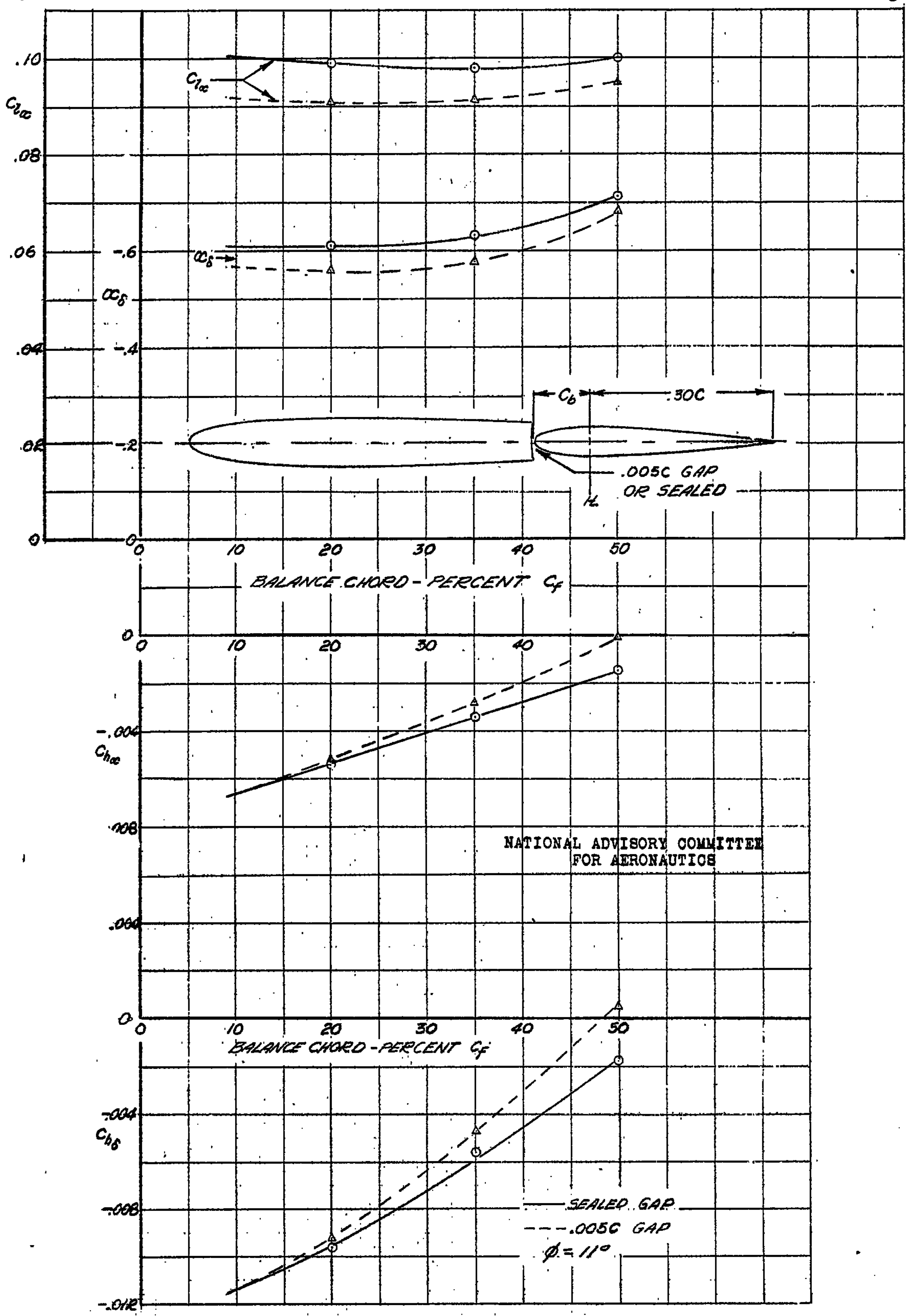


FIGURE 1.- THE VARIATION OF SECTION PARAMETERS WITH AERODYNAMIC BALANCE FOR AN NACA 0009 AIRFOIL EQUIPPED WITH A 0.30-CHORD FLAP WITH A MEDIUM NOSE PROFILE. ADAPTED FROM REF. 2, 3, 4, AND 5.

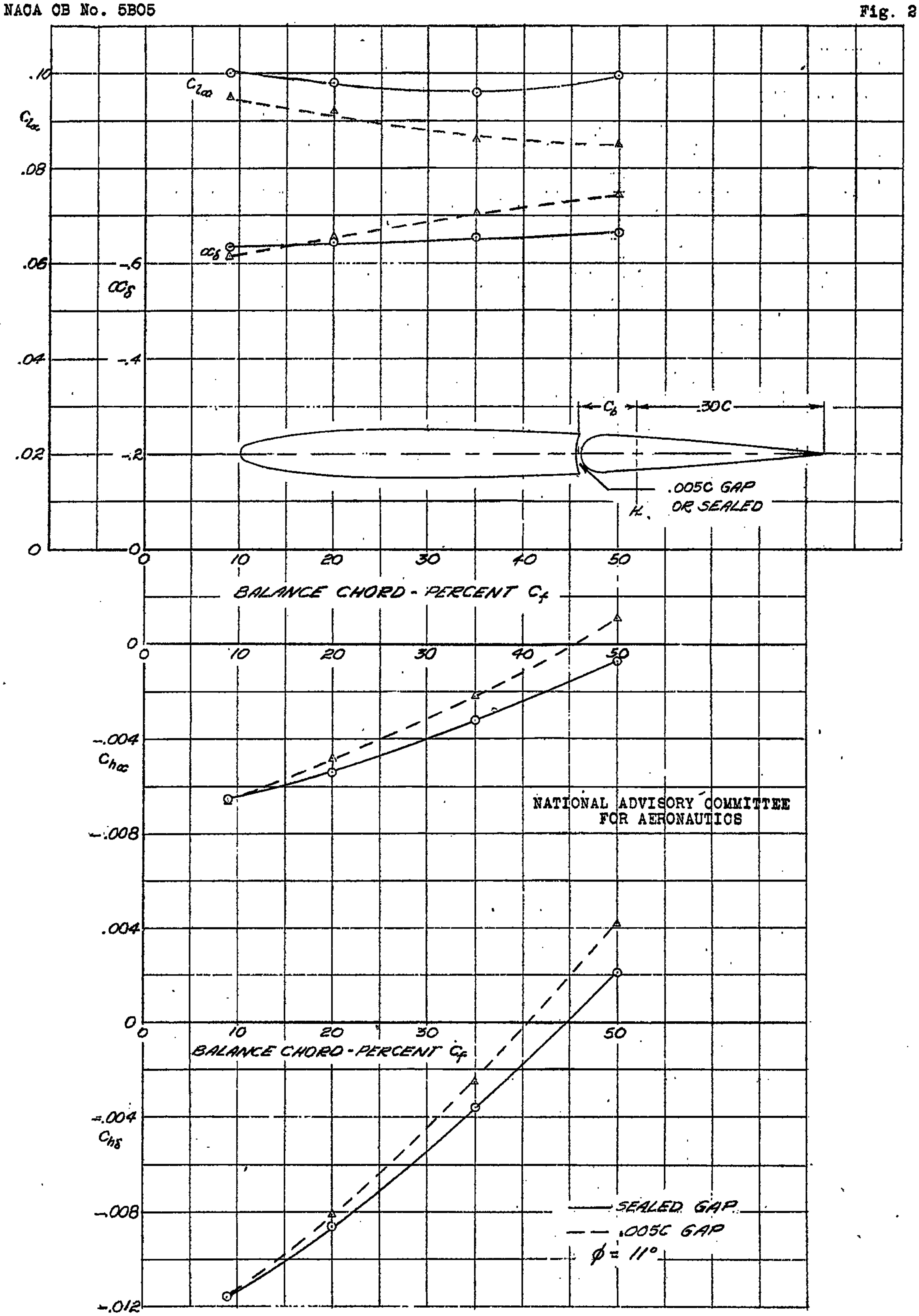


FIGURE 2.- THE VARIATION OF SECTION PARAMETERS WITH AERODYNAMIC BALANCE FOR AN NACA 0009 AIRFOIL EQUIPPED WITH A 0.30-CHORD FLAP WITH A BLUNT NOSE PROFILE. ADAPTED FROM REF. 2,3,4, AND 5.

A-11

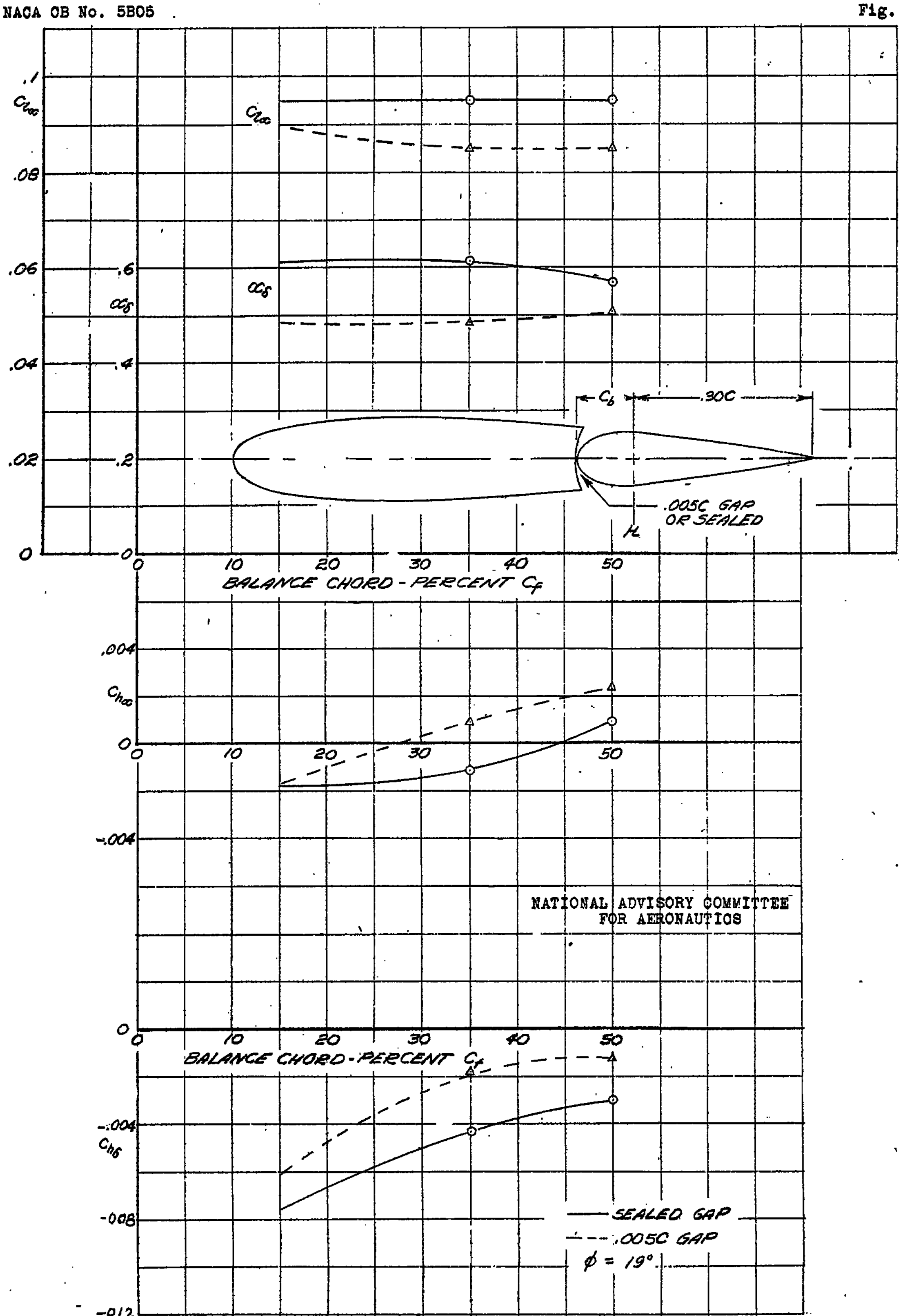


FIGURE 3.- THE VARIATION OF SECTION PARAMETERS WITH AERODYNAMIC BALANCE FOR AN NACA 0015 AIRFOIL EQUIPPED WITH A 0.30-CHORD FLAP WITH A MEDIUM NOSE PROFILE. ADAPTED FROM REF 6,7 AND 8.

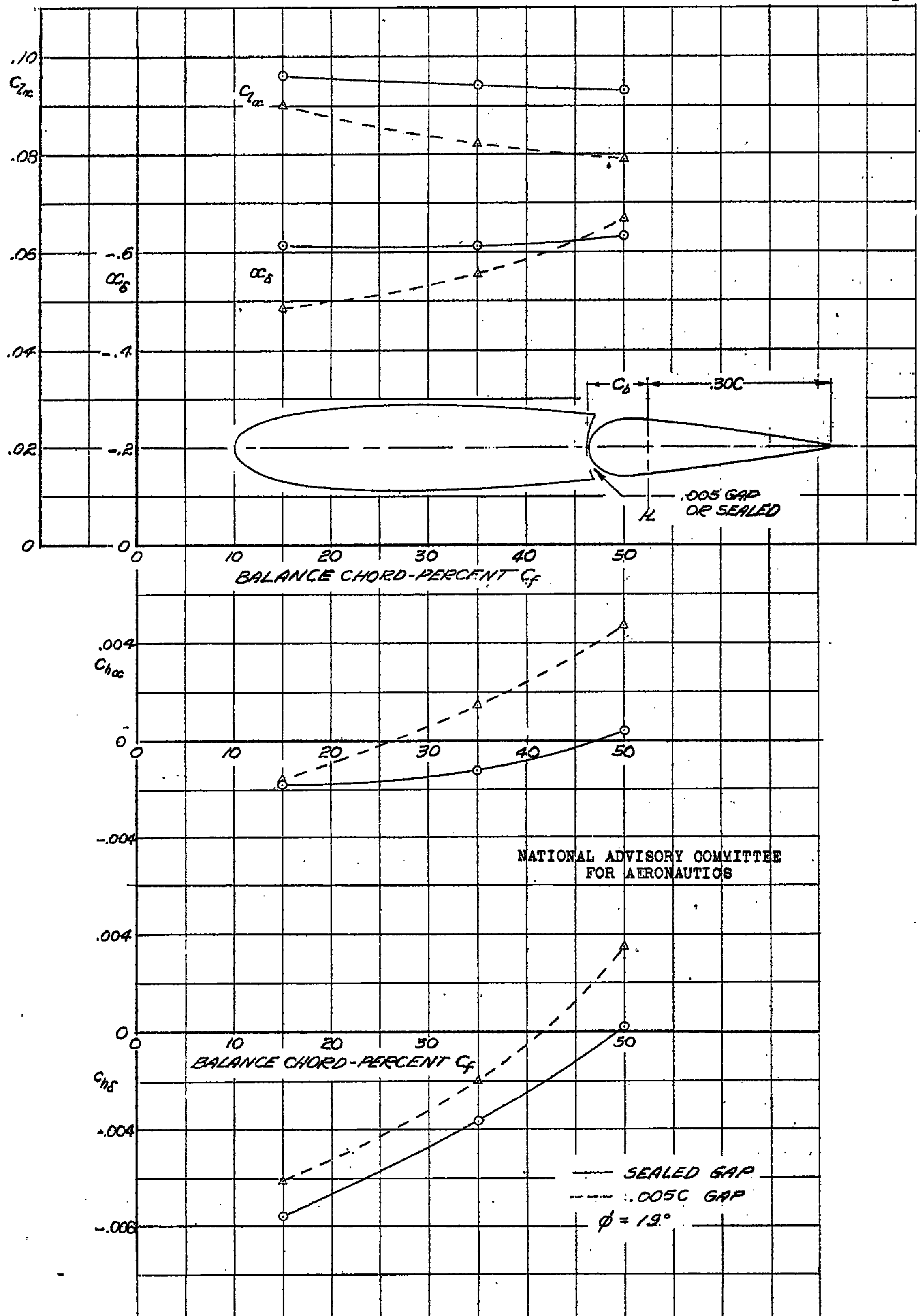


FIGURE 4.- THE VARIATION OF SECTION PARAMETERS WITH AERODYNAMIC BALANCE FOR AN NACA 0015 AIRFOIL EQUIPPED WITH A 0.30-CHORD FLAP WITH A BLUNT NOSE PROFILE. ADAPTED FROM REF. 6, 7, AND 8.

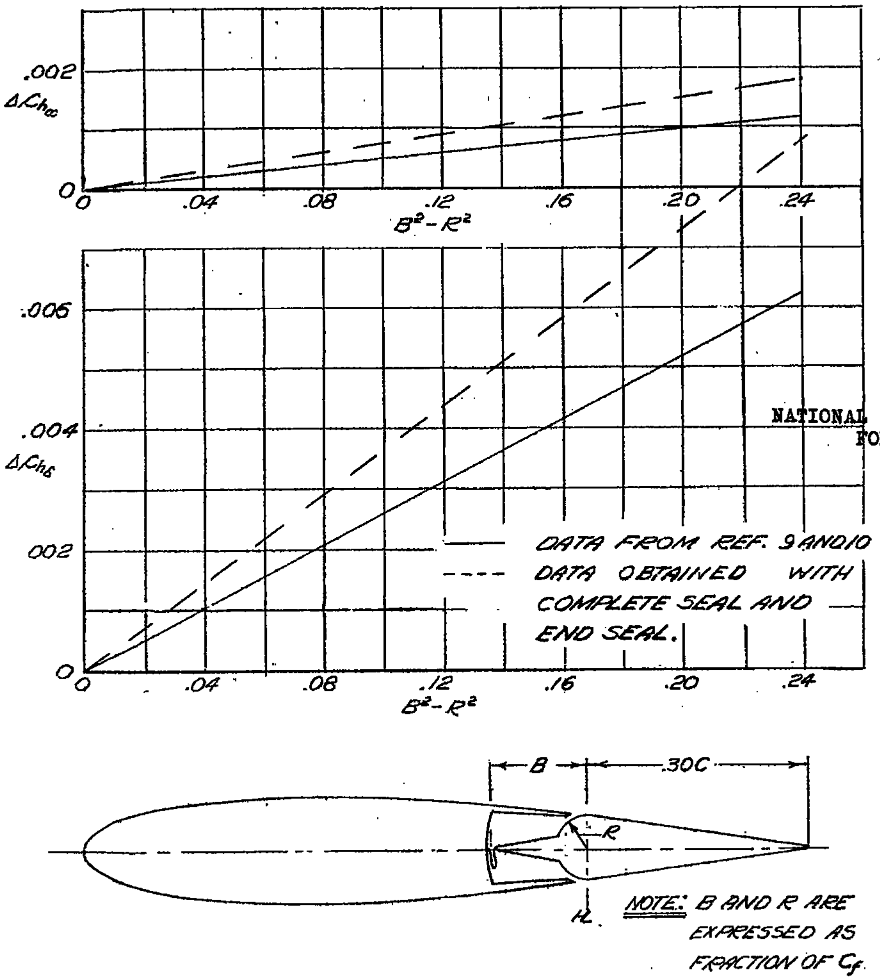


NATIONAL ADVISORY COMMITTEE FOR AERONAUTICS

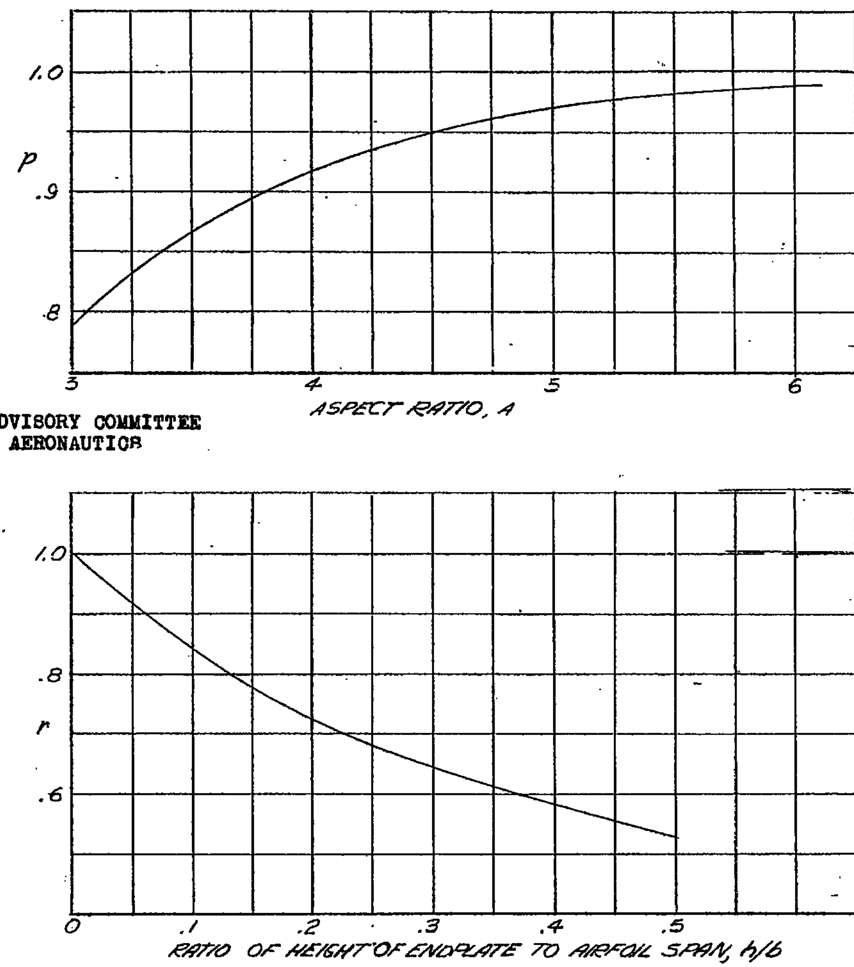


FIGURE 5.- THE VARIATION OF SECTION HINGE-MOMENT PARAMETERS WITH AERODYNAMIC BALANCE FOR AN NACA 0015 AIRFOIL EQUIPPED WITH A 0.30-CHORD FLAP OF STRAIGHT-SIDED PROFILE WITH SEALED, INTERNAL BALANCE.

FIGURE 8.- PARAMETERS $p$ AND $r$ FOR CORRECTION OF $C_{L_\alpha}$

$$C_{L_\alpha} = p\,\frac{c_{l_\alpha}}{1+\frac{57.3\, r\, c_{l_\alpha}}{\pi A}}$$

(FROM REF. 1)

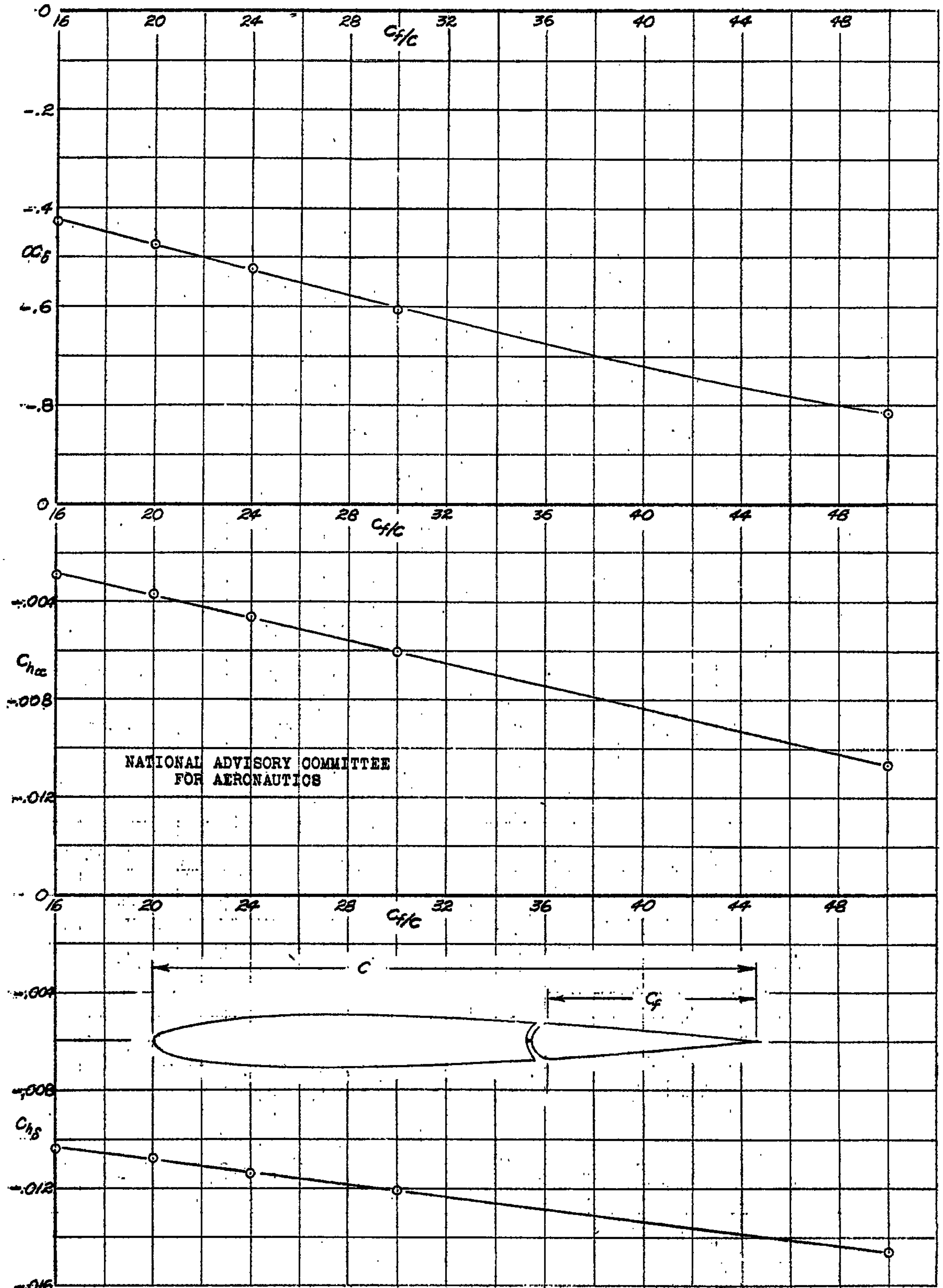


FIGURE 6.- THE VARIATION OF SECTION PARAMETERS WITH CONTROL-SURFACE CHORD FOR AN NACA 0009 AIRFOIL EQUIPPED WITH A PLAIN SEALED FLAP FROM REFERENCE 1.

A-11

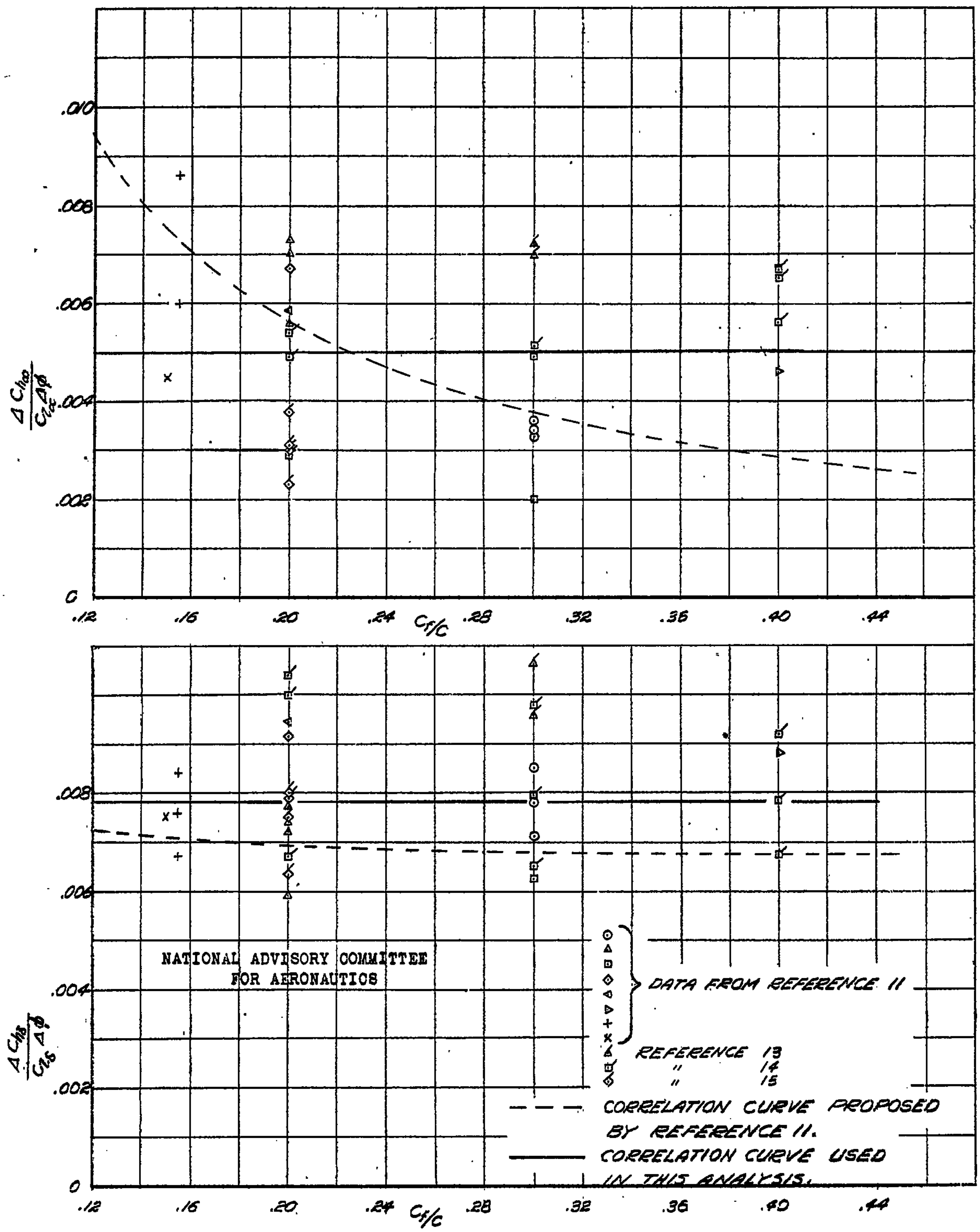


FIGURE 7.- THE VARIATION OF THE INCREMENTS OF THE SECTION HINGE-MOMENT PARAMETERS WITH CONTROL-SURFACE CHORD FOR A UNIT INCREMENT OF TRAILING-EDGE ANGLE

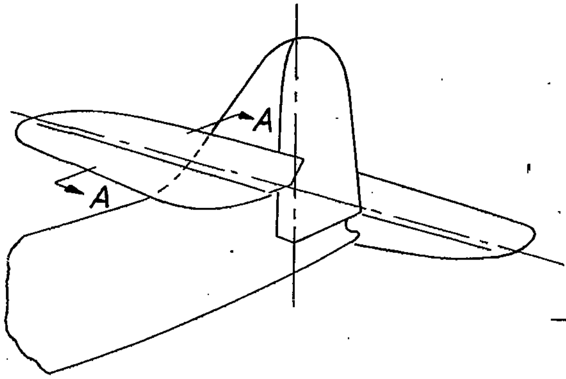


| | |
|---|---|
| $(\partial C_h/\partial \delta)_\alpha$ (CALCULATED) | -.0060 |
| $(\partial C_h/\partial \delta)_\alpha$ (EXPERIMENTAL) | -.0052 |
| $(\partial C_h/\partial \alpha)_\delta$ (CALCULATED) | -.0028 |
| $(\partial C_h/\partial \alpha)_\delta$ (EXPERIMENTAL) | -.0012 |
| $(\partial C_h/\partial C_m)_\alpha$ (CALCULATED) | .270 |
| $(\partial C_h/\partial C_m)_\alpha$ (EXPERIMENTAL) | .280 |

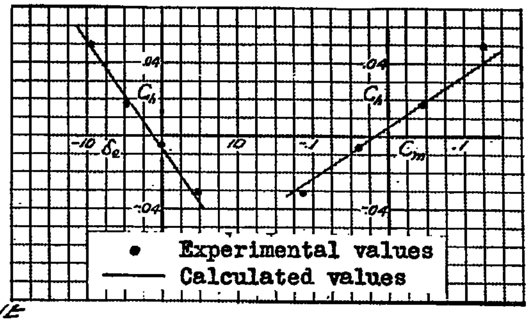


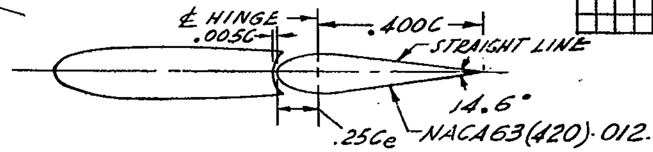


SECT A-A

NATIONAL ADVISORY COMMITTEE
FOR AERONAUTICS

FIGURE 9. – AIRPLANE A.

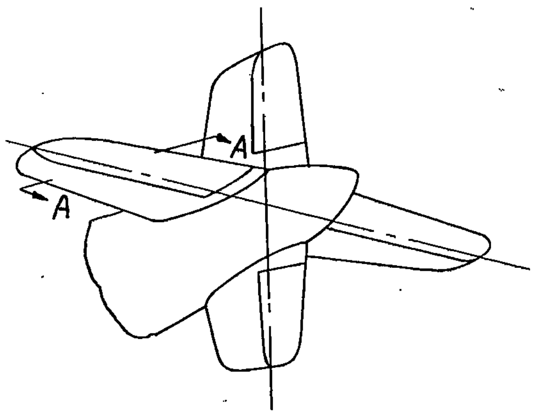


| | |
|---|---|
| $(\partial C_h/\partial \delta)_\alpha$ (CALCULATED) | -.0061 |
| $(\partial C_h/\partial \delta)_\alpha$ (EXPERIMENTAL) | -.0060 |
| $(\partial C_h/\partial \alpha)_\delta$ (CALCULATED) | -.0019 |
| $(\partial C_h/\partial \alpha)_\delta$ (EXPERIMENTAL) | -.0024 |
| $(\partial C_h/\partial C_m)_\alpha$ (CALCULATED) | .296 |
| $(\partial C_h/\partial C_m)_\alpha$ (EXPERIMENTAL) | .256 |

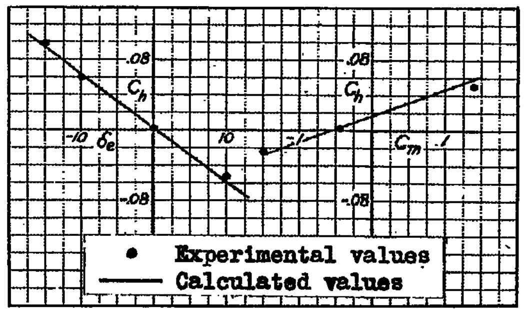


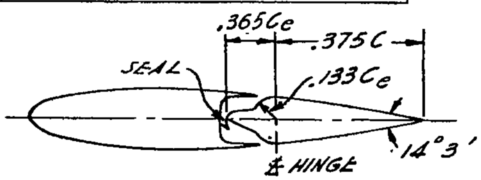


SECT. A-A

FIGURE 10. – AIRPLANE B.

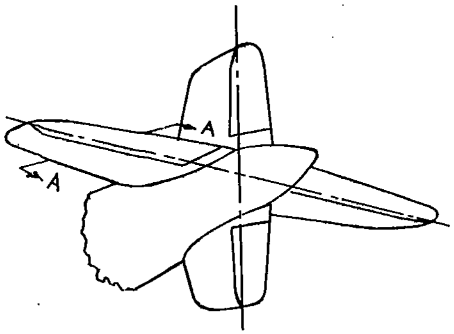


| | |
|---|---|
| $(\partial C_h/\partial \delta)_\alpha$ (CALCULATED) | −.0031 |
| $(\partial C_h/\partial \delta)_\alpha$ (EXPERIMENTAL) | −.0018 |
| $(\partial C_h/\partial \alpha)_\delta$ (CALCULATED) | −.0014 |
| $(\partial C_h/\partial \alpha)_\delta$ (EXPERIMENTAL) | −.0023 |
| $(\partial C_h/\partial C_m)_\alpha$ (CALCULATED) | .150 |
| $(\partial C_h/\partial C_m)_\alpha$ (EXPERIMENTAL) | .071 |

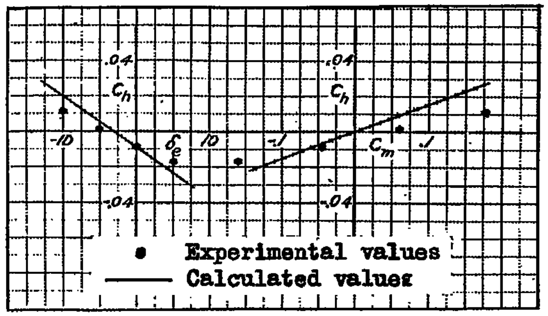


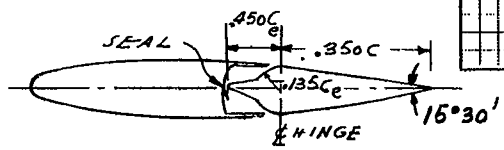


NATIONAL ADVISORY COMMITTEE
FOR AERONAUTICS

SECT. A-A

FIGURE 11.- AIRPLANE C

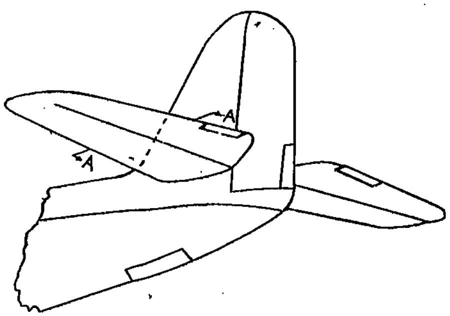


| | |
|---|---|
| $(\partial C_h/\partial \delta)_\alpha$ (CALCULATED) | −.0051 |
| $(\partial C_h/\partial \delta)_\alpha$ (EXPERIMENTAL) | −.0038 |
| $(\partial C_h/\partial \alpha)_\delta$ (CALCULATED) | −.0020 |
| $(\partial C_h/\partial \alpha)_\delta$ (EXPERIMENTAL) | 0 |
| $(\partial C_h/\partial C_m)_\alpha$ (CALCULATED) | .213 |
| $(\partial C_h/\partial C_m)_\alpha$ (EXPERIMENTAL) | .200 |

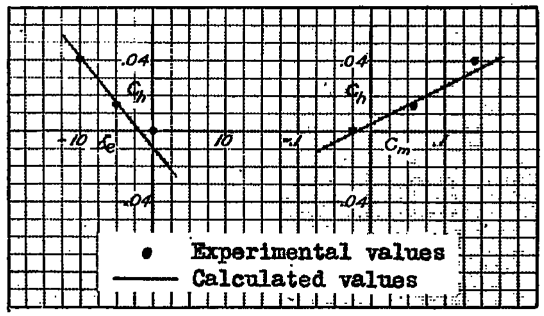


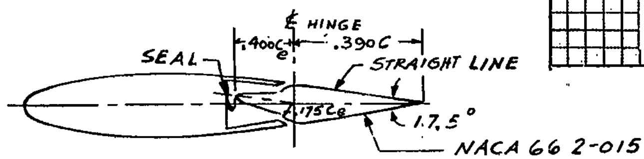


SECT A-A

FIGURE 12.-AIRPLANE D.

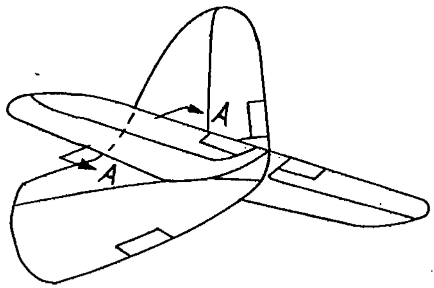


| | |
|---|---|
| $(\partial C_h/\partial \delta)_\alpha$ (CALCULATED) | $-.0024$ |
| $(\partial C_h/\partial \delta)_\alpha$ (EXPERIMENTAL) | $-.0016$ |
| $(\partial C_h/\partial \alpha)_\delta$ (CALCULATED) | $-.0009$ |
| $(\partial C_h/\partial \alpha)_\delta$ (EXPERIMENTAL) | $-.0002$ |
| $(\partial C_h/\partial C_m)_\alpha$ (CALCULATED) | .119 |
| $(\partial C_h/\partial C_m)_\alpha$ (EXPERIMENTAL) | .085 |

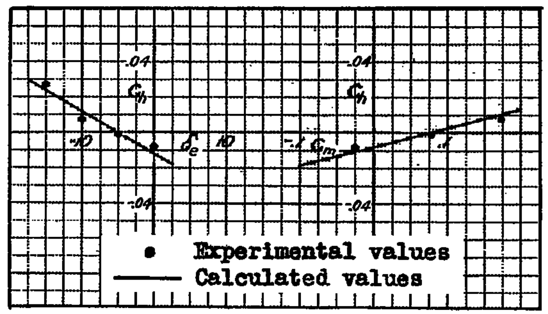


NATIONAL ADVISORY COMMITTEE
FOR AERONAUTICS

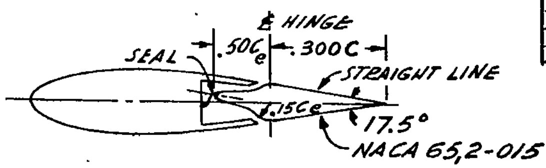


SECT. A-A

FIGURE 13.- AIRPLANE E.

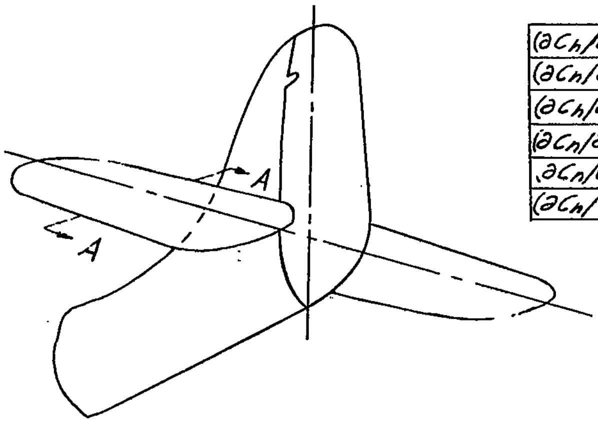


| | |
|---|---|
| $(\partial C_h/\partial \delta)_\alpha$ (CALCULATED) | $-.0027$ |
| $(\partial C_h/\partial \delta)_\alpha$ (EXPERIMENTAL) | $-.0029$ |
| $(\partial C_h/\partial \alpha)_\delta$ (CALCULATED) | $-.0010$ |
| $(\partial C_h/\partial \alpha)_\delta$ (EXPERIMENTAL) | $-.0010$ |
| $(\partial C_h/\partial C_m)_\alpha$ (CALCULATED) | .152 |
| $(\partial C_h/\partial C_m)_\alpha$ (EXPERIMENTAL) | .150 |

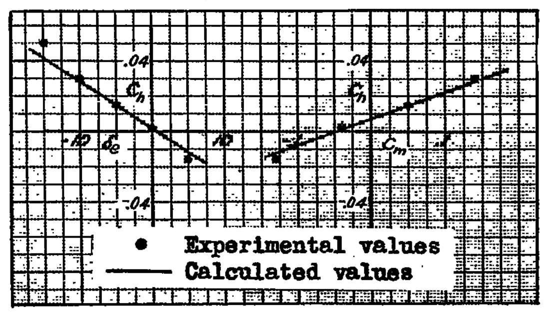


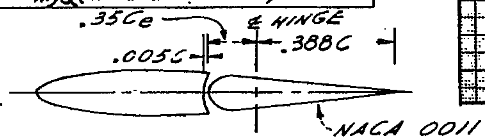


SECT. A-A

FIGURE 14.- AIRPLANE F.

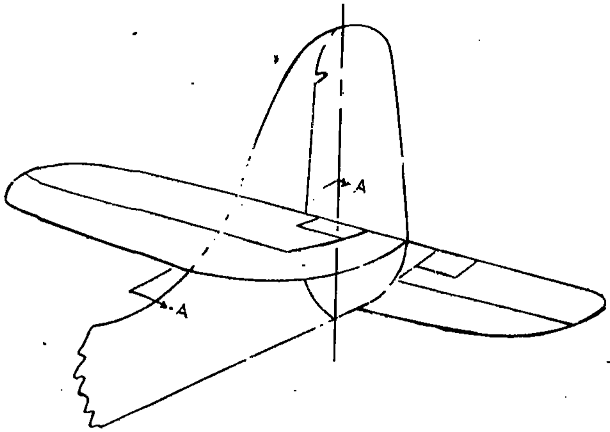


| | |
|---|---|
| $(\partial C_h/\partial \delta)_\alpha$ (CALCULATED) | -.0024 |
| $(\partial C_h/\partial \delta)_\alpha$ (EXPERIMENTAL) | -.0024 |
| $(\partial C_h/\partial \alpha)_\delta$ (CALCULATED) | -.0009 |
| $(\partial C_h/\partial \alpha)_\delta$ (EXPERIMENTAL) | -.0006 |
| $(\partial C_h/\partial C_m)_\alpha$ (CALCULATED) | .130 |
| $(\partial C_h/\partial C_m)_\alpha$ (EXPERIMENTAL) | .130 |

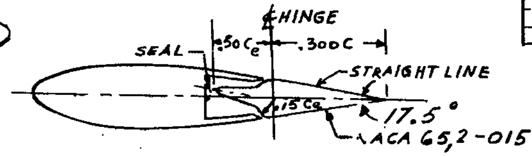


SECT A-A

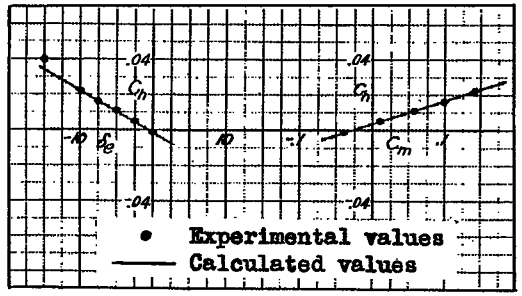


NATIONAL ADVISORY COMMITTEE
FOR AERONAUTICS

FIGURE 15.- AIRPLANE G.

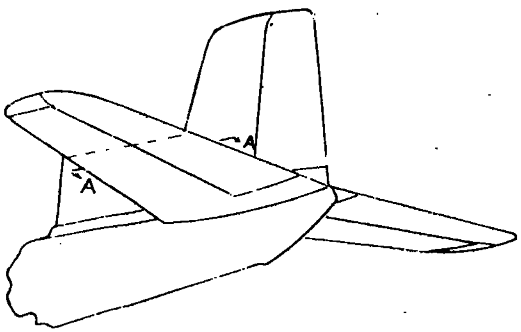


| | |
|---|---|
| $(\partial C_h/\partial \delta)_\alpha$ (CALCULATED) | -.0054 |
| $(\partial C_h/\partial \delta)_\alpha$ (EXPERIMENTAL) | -.0043 |
| $(\partial C_h/\partial \alpha)_\delta$ (CALCULATED) | -.0021 |
| $(\partial C_h/\partial \alpha)_\delta$ (EXPERIMENTAL) | -.0010 |
| $(\partial C_h/\partial C_m)_\alpha$ (CALCULATED) | .303 |
| $(\partial C_h/\partial C_m)_\alpha$ (EXPERIMENTAL) | .270 |

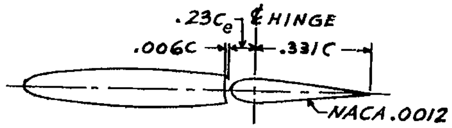


SECT. A-A

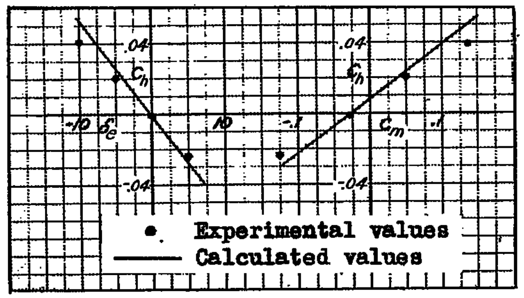


FIGURE 16.- AIRPLANE H.

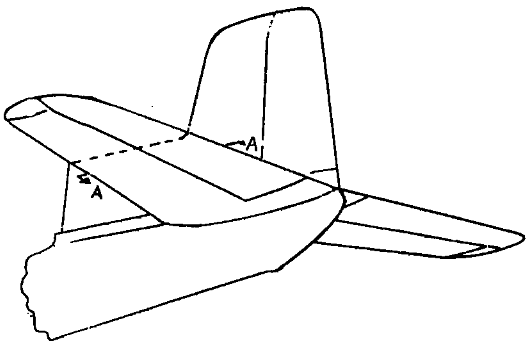


| | |
|---|---|
| $(\partial C_h/\partial \delta)_\alpha$ (CALCULATED) | -.0049 |
| $(\partial C_h/\partial \delta)_\alpha$ (EXPERIMENTAL) | -.0036 |
| $(\partial C_h/\partial \alpha)_\delta$ (CALCULATED) | -.0018 |
| $(\partial C_h/\partial \alpha)_\delta$ (EXPERIMENTAL) | .0008 |
| $(\partial C_h/\partial C_m)_\alpha$ (CALCULATED) | .280 |
| $(\partial C_h/\partial C_m)_\alpha$ (EXPERIMENTAL) | .245 |

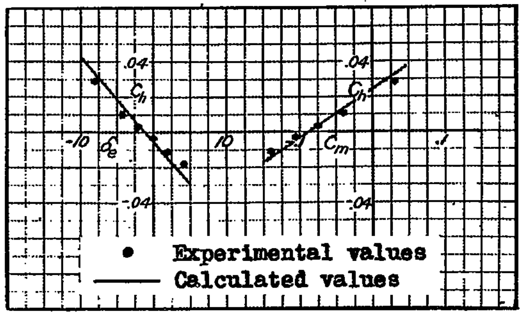


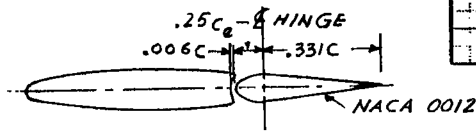


SECT. A-A

NATIONAL ADVISORY COMMITTEE
FOR AERONAUTICS

FIGURE 17.- AIRPLANE J.

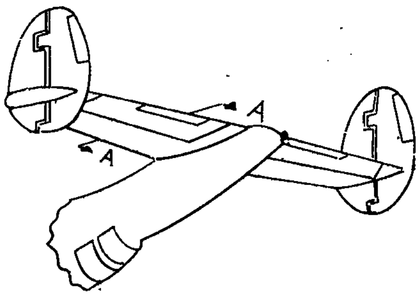


| | |
|---|---|
| $(\partial C_h/\partial \delta)_\alpha$ (CALCULATED) | -.0094 |
| $(\partial C_h/\partial \delta)_\alpha$ (EXPERIMENTAL) | -.0086 |
| $(\partial C_h/\partial \alpha)_\delta$ (CALCULATED) | -.0043 |
| $(\partial C_h/\partial \alpha)_\delta$ (EXPERIMENTAL) | -.0026 |
| $(\partial C_h/\partial C_m)_\alpha$ (CALCULATED) | .360 |
| $(\partial C_h/\partial C_m)_\alpha$ (EXPERIMENTAL) | .305 |

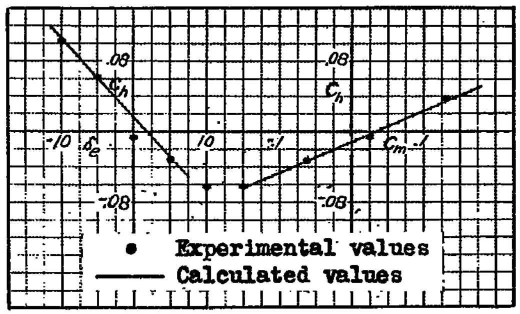


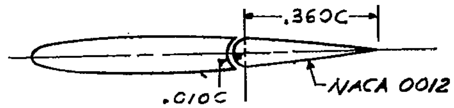


SECT. A-A

FIGURE 18.- AIRPLANE K.

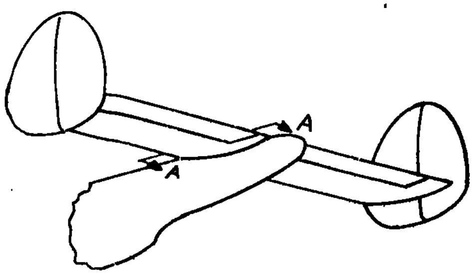


NATIONAL ADVISORY COMMITTEE
FOR AERONAUTICS

| | |
|---|---|
| $(\partial C_h/\partial \delta)_\alpha$ (CALCULATED) | −.0050 |
| $(\partial C_h/\partial \delta)_\alpha$ (EXPERIMENTAL) | −.0054 |
| $(\partial C_h/\partial \alpha)_\delta$ (CALCULATED | −.0010 |
| $(\partial C_h/\partial \alpha)_\delta$ (EXPERIMENTAL) | −.0002 |
| $(\partial C_h/\partial C_m)_\alpha$ (CALCULATED) | .304 |
| $(\partial C_h/\partial C_m)_\alpha$ (EXPERIMENTAL) | .364 |

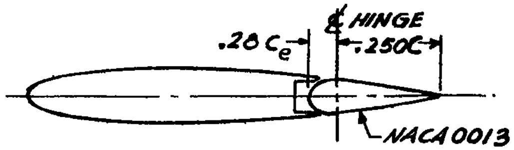


SECT. A-A

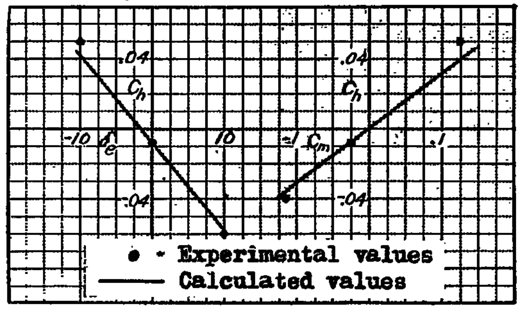


FIGURE 19.- AIRPLANE L.

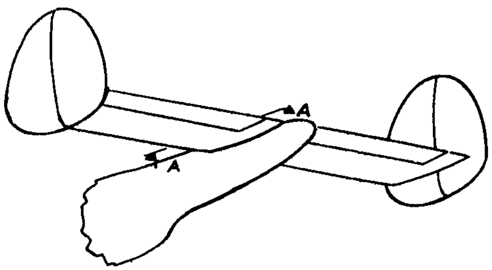


| | |
|---|---|
| $(\partial C_h/\partial \delta)_\alpha$ (CALCULATED) | −.0024 |
| $(\partial C_h/\partial \delta)_\alpha$ (EXPERIMENTAL) | −.0032 |
| $(\partial C_h/\partial \alpha)_\delta$ (CALCULATED) | −.0002 |
| $(\partial C_h/\partial \alpha)_\delta$ (EXPERIMENTAL) | 0 |
| $(\partial C_h/\partial C_m)_\alpha$ (CALCULATED) | .134 |
| $(\partial C_h/\partial C_m)_\alpha$ (EXPERIMENTAL) | .200 |

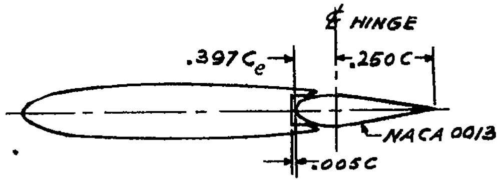


SECT. A-A

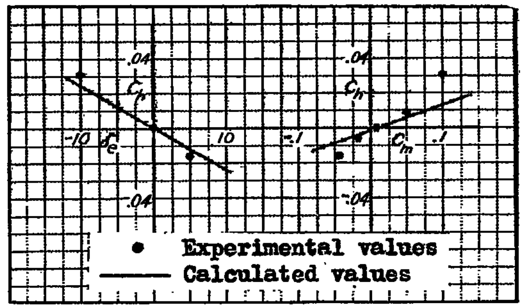


FIGURE 20.- AIRPLANE M

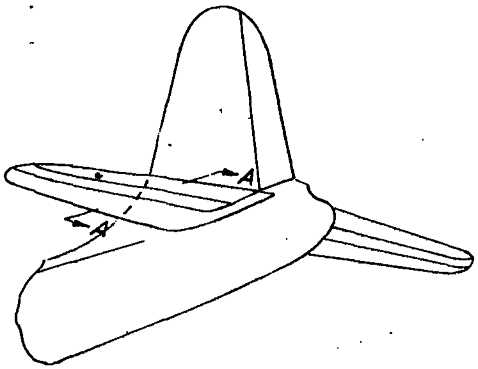


NATIONAL ADVISORY COMMITTEE
FOR AERONAUTICS

| | |
|---|---|
| $(\partial C_h/\partial \delta)_\alpha$ (CALCULATED) | -.0066 |
| $(\partial C_h/\partial \delta)_\alpha$ (EXPERIMENTAL) | -.0063 |
| $(\partial C_h/\partial \alpha)_\delta$ (CALCULATED) | -.0007 |
| $(\partial C_h/\partial \alpha)_\delta$ (EXPERIMENTAL) | .0008 |
| $(\partial C_h/\partial C_m)_\alpha$ (CALCULATED) | .306 |
| $(\partial C_h/\partial C_m)_\alpha$ (EXPERIMENTAL) | .500 |

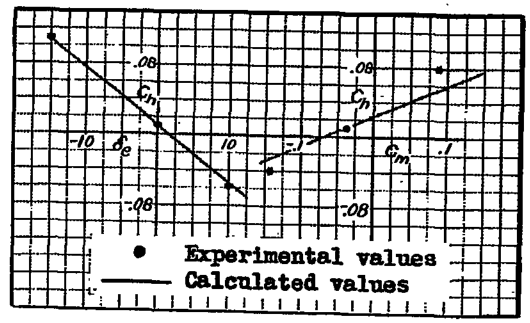


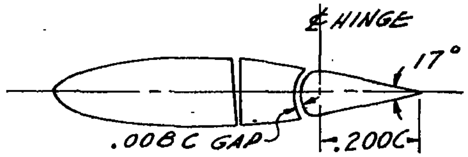


SECT. A-A

FIGURE 21 - AIRPLANE N.

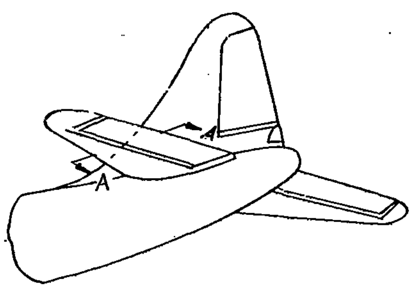


| | |
|---|---|
| $(\partial C_h/\partial \delta)_\alpha$ (CALCULATED) | .0002 |
| $(\partial C_h/\partial \delta)_\alpha$ (EXPERIMENTAL) | .0002 |
| $(\partial C_h/\partial \alpha)_\delta$ (CALCULATED) | .0008 |
| $(\partial C_h/\partial \alpha)_\delta$ (EXPERIMENTAL) | .0007 |
| $(\partial C_h/\partial C_m)_\alpha$ (CALCULATED) | -.008 |
| $(\partial C_h/\partial C_m)_\alpha$ (EXPERIMENTAL) | 000 |

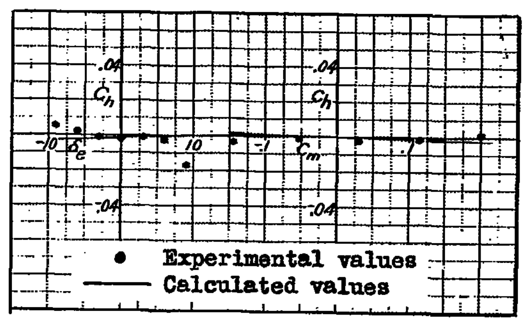


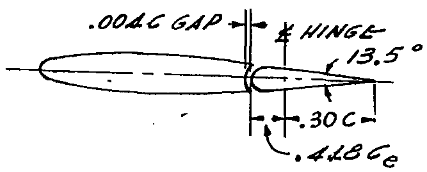


SECT A-A

FIGURE 22.-AIRPLANE O.

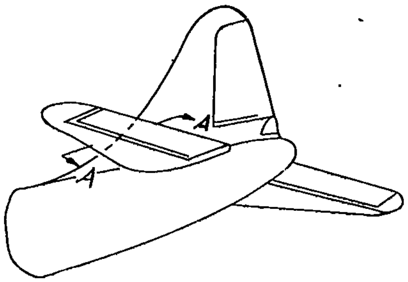


| | |
|---|---|
| $(\partial C_h/\partial \delta)_\alpha$ (CALCULATED) | .0025 |
| $(\partial C_h/\partial \delta)_\alpha$ (EXPERIMENTAL) | .0032 |
| $(\partial C_h/\partial C_m)_\alpha$ (CALCULATED) | −.103 |
| $(\partial C_h/\partial C_m)_\alpha$ (EXPERIMENTAL) | −.130 |

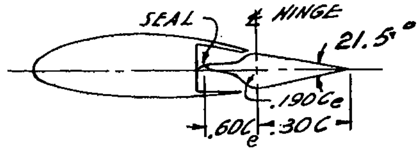


SECT. A-A

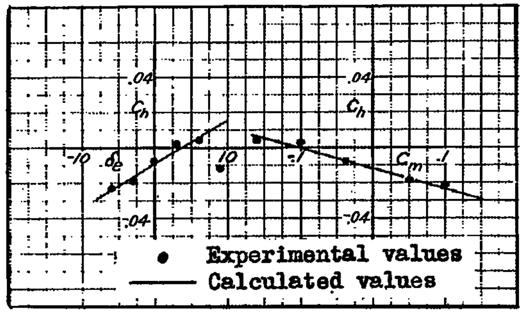


NATIONAL ADVISORY COMMITTEE
FOR AERONAUTICS

FIGURE 23.- AIRPLANE P

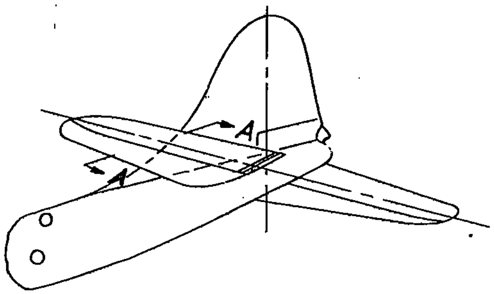


| | |
|---|---|
| $(\partial C_h/\partial \delta)_\alpha$ (CALCULATED) | −.0011 |
| $(\partial C_h/\partial \delta)_\alpha$ (EXPERIMENTAL) | −.0010 |
| $(\partial C_h/\partial \alpha)_\delta$ (CALCULATED) | −.0019 |
| $(\partial C_h/\partial \alpha)_\delta$ (EXPERIMENTAL) | −.0006 |

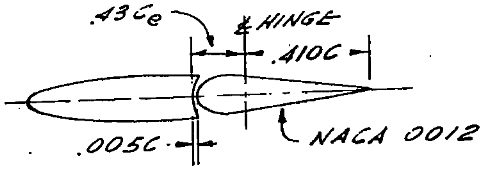


SECT. A-A

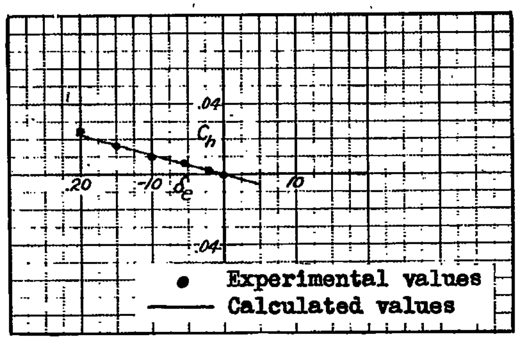


FIGURE 24.- AIRPLANE Q